Quantum Pyragas control: Selective control of individual photon probabilities

Leon Droenner, Nicolas L. Naumann, Eckehard Schöll, Andreas Knorr, and Alexander Carmele*
Technische Universität Berlin, Institut für Theoretische Physik, Hardenbergstraße 36, 10623 Berlin, Germany

(Received 12 January 2018; published 21 February 2019)

Pyragas control allows us to stabilize unstable states in applied nonlinear science. We propose to apply a quantum version of the Pyragas protocol to control individual photon probabilities in an otherwise only globally accessible photon-probability distribution of a quantum light emitter. The versatility of quantum Pyragas control is demonstrated for the case of a two-level emitter in a pulsed laser-driven half cavity. We show that one- and two-photon events respond in a qualitatively different way to the half-cavity-induced feedback signal. One-photon events are either enhanced or suppressed, depending on the choice of parameters. In contrast, two-photon events undergo exclusively an enhancement up to 50% for the chosen pulse areas. We hereby propose an implementation of quantum Pyragas control via a time-delayed feedback setup.

DOI: 10.1103/PhysRevA.99.023840

I. INTRODUCTION

Since its introduction, the delayed feedback control method [1,2] is still one of the most active fields in applied nonlinear science [3–6]. Pyragas control is a specific form of such a closed-loop feedback control protocol which allows one to force noninvasively a system into a desired target state and vanishes as soon as this state is attained [7]. Being reference-signal-free the controlled system can be treated as a black box as no exact knowledge of either the form of the periodic orbit or the system of equations is needed. A standard (classical) Pyragas control takes the following form:

$$\dot{x}(t) = f(x(t), t) - K[x(t) - x(t-\tau)]. \tag{1}$$

Hence, whenever the delay τ is an integer multiple of the period of the target solution $x(t) = x(t+\tau)$ of the uncontrolled nonlinear system $\dot{x} = f(x)$, the solution persists and the control force K vanishes on the target orbit. Successful experimental implementations of the Pyragas method include, e.g., control of unstable orbits in a CO_2 laser with modulated losses [8] and a wide range of applications in semiconductor laser systems [9–13]. In electronic systems, time-delayed feedback is applied to enforce autosynchronization in diode resonators [14,15], is applied in chemical systems to control chaos in Belousov-Zhabotinsky reactions [16], and addresses birhythmicity in physical, biological systems in a noninvasive way [17,18]. In the physics of plasmas, the Pyragas method has been employed to control current-driven ion acoustic instabilities [19] and unstable low-frequency electrostatic waves arising from strong modulations of ion and electron densities [20].

Despite the successes in semiclassical and classical nonlinear systems, feedback control in the quantum regime has been mostly investigated only in open-loop control, i.e., measurement-based protocols [21,22] with successes, e.g., in Fock-state preparation in microwave-cavity QED platforms [23] or persistent control of superconducting qubits [24]. Lately, considerable interest has shifted to closed-loop feedback control [25,26], and based on various theoretical models [27–30] predictions include stabilization of Rabi oscillations in the presence of a structured reservoir [27], control of unstable branches of bistable optomechanical systems [31–33], synchronization of network nodes [29,34–36], enhancement of polarization entanglement in a biexciton cascade [37], antibunching in multiphoton cavity QED [38], and squeezing in parametric oscillators [39,40]. In addition to these examples, we propose here a completely novel type of quantum control, allowing one to stabilize a single photon-probability in the photon-probability distribution of a quantum light emitter without changing neighboring probabilities.

The system we propose is based on all-optical quantum feedback of a two-level system (TLS) which is driven by an external pulsed laser field (cf. Fig. 1) and in which the pulse area controls the emission characteristics. To trigger single-photon emission, the Gaussian pulse inverts the TLS (π pulse), and a single photon is emitted subsequently due to radiative relaxation. However, if a 2π pulse is applied, the TLS favors a two-photon emission as has been demonstrated lately theoretically and experimentally [41–43]. The goal of this study is to demonstrate that Pyragas quantum feedback control is able to selectively suppress, enhance, and mediate between one- and two-photon emission events. Selective control here means that non-Markovian feedback allows one to enhance a single photon-probability without affecting other photon probabilities.

Typical measurement-based quantum control is modeled via a Lindblad-type jump operator acting on the full system density matrix $\mathcal{D}[J]\rho = 2J\rho J^\dagger - \{J^\dagger J, \rho\}$. Given a Markovian system-environment coupling, the dynamics of a single photon-probability $p(n) = \langle n|\rho|n\rangle$ with photon annihilation and creation operators b and $b^\dagger$, respectively, and decay constant κ reads as follows:

$$\dot{p}(n)/\kappa = \langle n|\mathcal{D}[b]\rho|n\rangle = -2np(n) + 2(n+1)p(n+1),$$

*alex@itp.tu-berlin.de

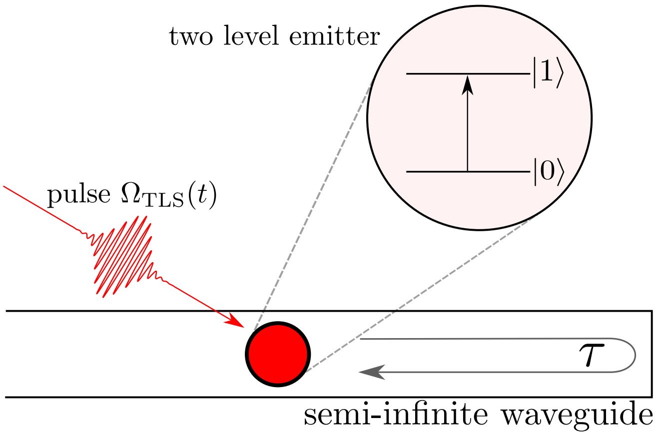

FIG. 1. Illustration of the system under pulsed excitation where a single TLS is placed inside a waveguide. A photon propagating to the right side is reflected and may excite the TLS again with delay τ.

in which necessarily the photon probabilities couple to each other due to the quantum jump part of the Lindblad operator. In contrast, as we demonstrate now, in a non-Markovian quantum control setup we are able to address just a single photon-probability and thus enhance $p(n)$ without influencing $p(n+1)$ or $p(n-1)$. We hereby expand the potential range of Pyragas control based on its quantum regime analog:

$$\dot{x}(t) = \frac{i}{\hbar}[H_s, x(t)] - K[x(t) - e^{i\phi}x(t-\tau)] + N(t), \tag{2}$$

for the Heisenberg operator $x(t)$ and $t > \tau$ with system dynamics induced by the system's Hamiltonian H_s and the Pyragas control contribution [27,30]. Note that the quantum version of Pyragas control includes inevitably a control phase parameter ϕ and due to the control environment a noise operator $N(t)$ to ascertain the conservation of the canonical commutation relation of $[x, p] = i\hbar$ [21].

As a physical implementation we have in mind a light-reflecting element (external mirror, integrated semi-infinite waveguide) which feeds the photons emitted by the system back into the system after a roundtrip of τ (cf. Fig. 1). This is a quantum version of the Lang-Kobayashi setup [44] and has already been realized in the quantum regime for cold atoms and semiconductor lasers [45,46]. Due to the mirror-induced boundary condition, the dynamics is essentially non-Markovian and due to the driving laser-field standard quantum optical methods fails to model the system. Here, we model the feedback with the quantum stochastic Schrödinger equation [21,29,47], where a matrix-product-state representation allows us to treat only the most relevant part of the Hilbert space corresponding to a numerically exact treatment [48,49].

II. QUANTUM PYRAGAS MODEL

We consider a single TLS with transition energy $\hbar\omega_0$ inside a semi-infinite waveguide [50,51] (cf. Fig. 1). A spontaneous decay of the electronic excited state induced by the lowering operator $\sigma_-|1\rangle = |0\rangle$ emits a photon into the waveguide. The waveguide is closed at the right side, for instance, by a reflecting cavity, acting as a mirror. We model the interaction between the waveguide and the TLS with the following quantum feedback-inducing Hamiltonian:

$$H_{\mathrm{fb}} = \hbar g_0 \int_{\mathcal{B}} d\omega[\sin(\omega L/c_0)b^\dagger(\omega)\sigma_- + \mathrm{H.a.}], \tag{3}$$

with $b^{(\dagger)}(\omega)$ being the annihilation (creation) operator for a waveguide photon of frequency ω and the raising or lowering operator for atomic excitation $\sigma_\pm$. The TLS-reservoir interaction is described by $G_{\mathrm{fb}}(\omega) = g_0 \sin(\omega L/c_0)$ [52,53], with c_0 being the speed of light in the waveguide. The coupling $G_{\mathrm{fb}}(\omega)$ includes the reflecting mirror at distance L from the TLS with time delay $\tau = 2L/c_0$ before an emitted photon again interacts with the TLS. This interaction Hamiltonian H_{fb} gives rise to the quantum Pyragas equation for a given waveguide photon or system operator in the Heisenberg picture [cf. Eq. (2)]:

$$\begin{aligned}\dot{\sigma}_-(t) = {}& \frac{i}{\hbar}[H_s, \sigma_-] - \Gamma\sigma_-(t) + N(t) \\ & + \Gamma e^{i\omega_0\tau}\sigma_-(t-\tau)\sigma_+(t)\sigma_-(t)\theta(t-\tau) \\ & - \Gamma e^{i\omega_0\tau}\sigma_-(t-\tau)\sigma_-(t)\sigma_+(t)\theta(t-\tau),\end{aligned} \tag{4}$$

where we have set $\Gamma = \pi g_0^2/2$ as the radiative decay constant and $N(t) = i\int_{\mathcal{B}} d\omega G_{\mathrm{fb}}(\omega) b_0^\dagger(\omega)\exp[-i\omega t]$ denotes the noise contribution which conserves the commutation relation and $b_0^\dagger(\omega)$ as the annihilation operator of a waveguide photon at $t = 0$. If $t > \tau$ and $\sigma_-(t) = \sigma_-(t-\tau)$, the equation of motion reduces to

$$\dot{\sigma}_-(t)|_{\mathrm{periodic}} = \frac{i}{\hbar}[H_s, \sigma_-] - \Gamma[1 + e^{i\omega_0\tau}]\sigma_-(t) + N(t),$$

and for specific phases $\phi = \omega_0\tau = n\pi$ for the n integer and negligible noise contributions, we recover the pure system dynamics governed by H_s as in the classical case. Due to the phase and quantum noise contributions, the quantum version of the Pyragas method offers new degrees of freedom beyond the control of periodic orbits. In the following, we show that exactly this phase via a given delay time allows us to address selectively a single photon-probability in the photon-probability distribution $p(n)$.

III. QUANTUM FEEDBACK IN THE MATRIX-PRODUCT-STATE PICTURE

We consider that the system dynamics is externally controlled via an external coherent pulse, resonant with the TLS frequency ω_0. As a control parameter, we choose the pulse area. The external laser is modeled as a Gaussian pulse with the frequency ω_L and the amplitude $\Omega(t) = A\, e^{-t^2/\nu^2}/\sqrt{\nu^2\pi}$, giving rise to the pulse area A in terms of the temporal width of the pulse ν. We choose the pulse to be short in comparison with the inverse decay rate of the electronic excited state Γ in the same manner as in Ref. [42]. For a longer pulse duration, the probabilities of higher photon numbers would become more relevant, which is beyond the scope of this present study. The total Hamiltonian reads $H_{\mathrm{tot}} = H_0 + H_{\mathrm{s}}(t) + H_{\mathrm{fb}}$, with

$$H_0 = \hbar\omega_0\sigma_+\sigma_- + \int_{\mathcal{B}} d\omega\hbar\omega b^\dagger(\omega)b(\omega) \tag{5}$$

and

$$H_{\mathrm{s}}(t) = \hbar\Omega(t)(\sigma_+ e^{-i\omega_{\mathrm{L}}t} + \sigma_- e^{i\omega_{\mathrm{L}}t}) \tag{6}$$

being the Hamiltonians of the pumped TLS in the energy-conserving rotating-wave and dipole approximations. Furthermore, we assume that an optimal pulse length minimizes additional decoherence [42] or that the time-dependent coherence of the quantum emitter is small in comparison to our investigated delay times τ [54].

The coupling to the reservoir in Hamiltonian (3) includes a sinusoidal dependence on the distance $\sin(\omega L/c_0)$. This is a non-Markovian feature induced by the reflecting mirror. Thus, for a simulation, a memory kernel of the non-Markovian reservoir is needed. To efficiently deal with the large Hilbert space, we model it within the quantum stochastic Schrödinger formalism, following Ref. [29]. The main idea is to discretize the time evolution into equidistant time steps $t_k = k\Delta t$ and $t_{k+1} - t_k = \Delta t$.

In order to define the time-discrete time-evolution operator from t_k to t_{k+1}, we transform the feedback Hamiltonian by introducing a rotating frame with ω_L (assuming resonant excitation $\omega_L = \omega_0$) and defining the time-dependent bath operators

$$b(t) = \frac{1}{\sqrt{2\pi}} \int_{-\infty}^{\infty} d\omega b(\omega) e^{-i(\omega-\omega_L)t}. \tag{7}$$

The Hamiltonians are then written as

$$\begin{aligned} H_{\mathrm{s,rf}}(t) &= \hbar\Omega(t)(\sigma_+ + \sigma_-), \\ H_{\mathrm{fb,rf}}(t) &= -i\hbar\left(\sqrt{\frac{\Gamma}{2}} b(t-\tau)e^{-i\phi} + \sqrt{\frac{\Gamma}{2}} b(t)\right)\sigma_+ + \mathrm{H.a.}, \end{aligned} \tag{8}$$

and the corresponding time-evolution operator from time t_k to t_{k+1} reads

$$U(t_{k+1}, t_k) = \hat{T}\left[\exp\left(-\frac{i}{\hbar}\int_{t_k}^{t_{k+1}} dt' H(t')\right)\right]. \tag{9}$$

In defining the photon-bin operators $\Delta B(t_k) = \int_{t_k}^{t_{k+1}} dt b(t)$, which only act on the time interval $t_{k+1} - t_k$, the time-ordering operator $\hat{T}$ becomes redundant. These photon-bin operators obey the commutation relations

$$[\Delta B(t_j), \Delta B^\dagger(t_k)] = \Delta t \delta_{j,k}, \tag{10}$$

and we introduce the basis states

$$|i_p\rangle = \frac{[\Delta B^\dagger(t_p)]^{i_p}}{\sqrt{i_p! \Delta t^{i_p}}} |\mathrm{vac}\rangle \tag{11}$$

in the same manner as in Ref. [29]. The Schrödinger wave function reads as follows in the new basis:

$$|\Psi\rangle = \sum_{\{i\}} \psi_{\ldots, i_k, i_S, \ldots, i_{k-l}, \ldots} |\ldots, i_k, i_S, i_{k-1}, \ldots, i_{k-l}, \ldots\rangle, \tag{12}$$

with coefficient $\Psi_{\ldots, i_k, i_S, \ldots, i_{k-l}, \ldots}$. However, for a time discretization of $\tau/\Delta t = 100$, where Δt is the numerical time step, and a maximal photon number $n = 4$ of the reservoir, this would correspond to a Hilbert space of approximately 3×10^{60} states for one τ-interval. To efficiently treat the time evolution, we decompose $|\Psi(t_k + 1)\rangle$ with a series of singular-value decompositions such that it can be written as a matrix product state. The singular values express the entanglement between the system and the reservoir. If singular values are sufficiently small, the state is truncated by neglecting these singular values and thus the matrix dimension is reduced [55]. After decomposing $|\Psi(t_k + 1)\rangle$, the coefficient reads

$$\psi_{\{i\}} = A^{[k]}_{i_k, \alpha_k} A^{[\mathrm{S}]}_{\alpha_k, i_S, \beta_\mathrm{S}} A^{[k-1]}_{\beta_\mathrm{S}, i_{k-1}, \beta_{k-1}} \ldots A^{[-l]}_{\beta_{-l}, i_{k-l}} \ldots, \tag{13}$$

where k is the future time-bin (with i_k being the physical index), S is the tensor of the system (with i_S being the physical index), and $k - l$ is the feedback time-bin (with i_{k-l} being the physical index). Thus, the tensors A represent either the photon bins or the system. All indices α_i and β_i correspond to links between the tensors. By writing the state of the system and the reservoir in such a way, one can cut the zero-value Schmidt coefficients and thus efficiently deal with a large Hilbert space. Initially, the state $|\Psi(0)\rangle$ represents the system in the ground state and the reservoir in a vacuum state.

Due to the pulsed excitation, it is beneficial to expand the time-evolution operator to a higher order in Δt to deal with the two different time scales of the pulsed excitation scheme. To write the Hamiltonian in Eq. (8) in matrix form, we use the basis $|i_S, i_n, i_\tau\rangle$, where i_S is the level of the TLS, i_n is the occupation of the photon bin at the current time step t_k, and i_τ is the occupation of the photon bin at time step $t_{k-l} = t_k - \tau$. With this, we get the system matrix:

$$\begin{aligned} \mathbf{M}_{\mathrm{TLS,env}}(t_n) &= \int_{t_k}^{t_{k+1}} \langle j_S, j_n, j_\tau | H_{\mathrm{TLS,rf}}(t) | i_S, i_n, i_\tau\rangle dt \\ &= \hbar\Delta t[\Omega(t_n)(\delta_{j_S,1}\delta_{i_S,0} + \delta_{j_S,0}\delta_{i_S,1})]\delta_{j_n,i_n}\delta_{j_\tau,i_\tau}. \end{aligned} \tag{14}$$

We assume the envelope function $\Omega(t)$ to be slowly varying in the time step Δt. Furthermore, we use that the system operators are not explicitly time dependent. The feedback reservoir matrix is obtained via

$$\begin{aligned} \mathbf{M}_{\mathrm{fb}} &= \frac{i}{\hbar\sqrt{\Delta t}} \int_{t_k}^{t_{k+1}} \langle j_S, j_n, j_\tau | H_{\mathrm{fb,rf}} | i_S, i_n, i_\tau\rangle dt \\ &= \left(\sqrt{\frac{\Gamma}{2}}\sqrt{i_\tau}\delta_{j_\tau+1,i_\tau} e^{-i\phi} + \sqrt{\frac{\Gamma}{2}}\sqrt{i_n}\delta_{j_n+1,i_n}\right)\delta_{j_S,1}\delta_{i_S,0} \\ &\quad - \left(\sqrt{\frac{\Gamma}{2}}\sqrt{j_\tau}\delta_{j_\tau,i_\tau+1} e^{-i\phi} + \sqrt{\frac{\Gamma}{2}}\sqrt{j_n}\delta_{j_n,i_n+1}\right)\delta_{j_S,0}\delta_{i_S,1}. \end{aligned} \tag{15}$$

We extract the time dependency of the pulsed excitation in order to deal with time-independent matrices of the system, defining the matrix $\mathbf{M}_{\mathrm{TLS}} = \mathbf{M}_{\mathrm{TLS,env}}(t_n)/\Omega(t_n)$. This has computational reasons as only the enveloping function $\Omega(t)$ changes with each time step. When evaluating the evolution matrix in higher order, all terms of Δt up to the desired order have to be taken into account in the expansion

$$\begin{aligned} \mathbf{U} &= \exp(\Omega(t_n)\mathbf{M}_{\mathrm{TLS}} + \mathbf{M}_{\mathrm{fb}}) \\ &= \sum_{p=0}^{\infty} \frac{1}{p!}(\Omega(t_n)\mathbf{M}_{\mathrm{TLS}} + \mathbf{M}_{\mathrm{fb}})^p. \end{aligned} \tag{16}$$

For the first-order evaluation in Δt, as used in Ref. [29], terms up to the order $p = 2$ in the expansion of $\mathbf{U}$ contribute, as $\mathbf{M}_{\mathrm{fb}} \propto \sqrt{\Delta t}$. Thus, for second-order expansion in Δt, terms up to $p = 4$ in Eq. (16) have to be considered. We use the expansion to second order which reads explicitly

$$\begin{aligned}\mathbf{U} &\approx \mathbf{U}_0 + \Omega(t)\mathbf{U}_1 + \Omega(t)^2\mathbf{U}_2\\ &= \mathbb{1} + \mathbf{M}_{\text{fb}} + \tfrac{1}{2}\mathbf{M}_{\text{fb}}^2 + \tfrac{1}{6}\mathbf{M}_{\text{fb}}^3 + \tfrac{1}{24}\mathbf{M}_{\text{fb}}^4\\ &\quad + \Omega(t_n)\big[\mathbf{M}_{\text{TLS}} + \tfrac{1}{2}(\mathbf{M}_{\text{TLS}}\mathbf{M}_{\text{fb}} + \mathbf{M}_{\text{fb}}\mathbf{M}_{\text{TLS}})\\ &\quad + \tfrac{1}{6}\big(\mathbf{M}_{\text{TLS}}\mathbf{M}_{\text{fb}}^2 + \mathbf{M}_{\text{fb}}\mathbf{M}_{\text{TLS}}\mathbf{M}_{\text{fb}} + \mathbf{M}_{\text{fb}}^2\mathbf{M}_{\text{TLS}}\big)\big]\\ &\quad + \Omega(t_n)^2\tfrac{1}{2}\mathbf{M}_{\text{TLS}}^2.\end{aligned} \tag{17}$$

The second line is the time-independent part of the evolution matrix $\mathbf{U}_0$, in the third and fourth lines the time dependence enters linearly and gives the linear part $\Omega(t_n)\mathbf{U}_1$. The last line is quadratic in the pump and gives the part $\Omega(t_n)^2\mathbf{U}_2$. With this, the time-evolution matrices of each order can be computed from the matrices $\mathbf{M}_{\text{fb}}$ and $\mathbf{M}_{\text{TLS}}$ by simple matrix multiplications. The enveloping function $\Omega(t)$ only needs to be evaluated once each time step. The time evolution of the system is evaluated by the sum

$$|\Psi(t_{k+1})\rangle = \big[\mathbf{U}_0 + \Omega(t)\mathbf{U}_1 + \Omega(t)^2\mathbf{U}_2\big]|\Psi(t_k)\rangle. \tag{18}$$

This can be simplified by saving the matrices $\mathbf{U}_i$ as sparse matrices so that the matrix multiplications are only marginally slower than for the time-independent evolution.

The greatest advantage in using a higher order in $U(t_{k+1}, t_k)$ is the larger possible step size $\Delta t = t_{k+1} - t_k$ with the same accuracy of the result. Thus, in total, less steps need to be performed. In addition, a single step needs fewer singular value decompositions as $l = \tau/\Delta t$ becomes smaller and results in a high speedup of the computation. A disadvantage of the higher order in $\mathbf{U}$ is that multiphoton processes become possible in a single time step. Thus, additional photon states in the time bins have to be taken into account. However, this additional complexity is outweighed by far by the speedup due to the reduction in singular value decompositions.

IV. SELECTIVE CONTROL OF PHOTON PROBABILITIES

Over a wide range of the pulse area A of the externally applied pulse, single-photon emission is the dominant process. However, at $A = 2n\pi$, where the excitation pulse induces full Rabi oscillations of the TLS, the two-photon probability $p(2)$ is higher than $p(1)$ [42,43]. During the excitation pulse, the TLS might decay and emit a photon. The remaining pulse re-excites the TLS and a second photon is emitted on a long timescale $1/\Gamma$. Our idea is to add an additional control parameter to steer the photon emission in this scenario and enhance just a single photon-probability, here $p(2)$.

Photon probabilities $p(n)$ are accessible via the time-integrated correlation functions:

$$\hat{I}^m = \left(\sum_{j=-\infty}^{\infty} \Delta B^\dagger(t_j)\Delta B(t_j)\right)^m. \tag{19}$$

To calculate the photon probabilities from the unnormalized time-integrated correlation functions [41], we use the Fock-state expansion of the photon density matrix:

$$C_m = \langle : \hat{I}^m : \rangle = \sum_{n=0}^{\infty} \frac{n!}{(n-m)!} p(n), \tag{20}$$

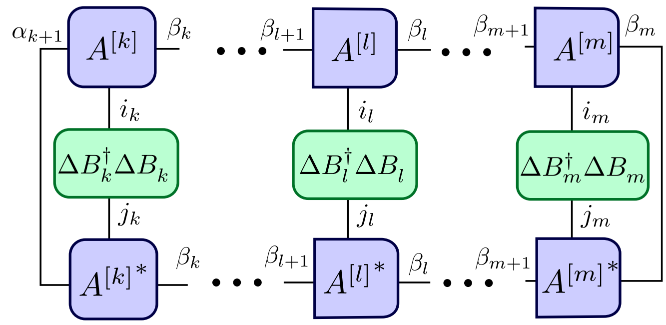

FIG. 2. Computation of one integrand of C_3 from the matrix product state in diagrammatic form. Round edges represent orthogonality. For each time combination, the intensity operator is applied at the corresponding time bins $A^{[\cdots]}$. The cost of this operation grows linearly with the difference $|k - m|$.

where ":" indicates the normal ordering of the operators, e.g.,

$$C_2 = \sum_{k=-q}^{N}\sum_{l=-q}^{N} \langle \Delta B^\dagger(t_k)\Delta B^\dagger(t_l)\Delta B(t_l)\Delta B(t_k)\rangle. \tag{21}$$

For the numerical evaluation, we note that there will be no light emitted into the environment before time $t = -\tau = -q\Delta t$, as we assume an initial vacuum state, and after a large enough time $t_{\text{end}} = N\Delta t$, all excitation from the TLS will be emitted into the bath, so that afterwards no photons will be observed. Assuming that $p(4)$ is negligible, we yield a closed set of equations:

$$p(1) = C_1 - C_2 + \frac{C_3}{2}, \tag{22a}$$

$$p(2) = \frac{C_2 - C_3}{2}, \tag{22b}$$

$$p(3) = C_3/6. \tag{22c}$$

We stay in pump regimes in which $p(3)$ is small compared to $p(1)$ and $p(2)$.This allows us to assume any correlations higher than third order to be negligible and justifies the cutoff in the expansion. Note that the correlation functions are nonlocal expectation values in time and are computed from the matrix product state after the time integration. Thus, for the computation of the correlation functions, we need a memory kernel for all integrated time steps. The computation algorithm for a single integrand of C_3 is depicted in Fig. 2 in diagrammatic form to give an example. The $A^{[\cdots]}$ tensors are time bins of the reservoir in canonical form [55] at the corresponding time step. According to the commutation relation in Eq. (10), the correlations are invariant under the reordering of the bath operators at different times. We can use this symmetry to reduce the cost of the numerical evaluation. We note that the higher order in $U(\Delta t)$ was obligatory for a numerically accessible computation of the third-order correlation function.

Having the photon-probabilities at hand, we can discuss the main result of this investigation with Fig. 3. The photon-probabilities for one- and two-photon events [$\bar{p}(1)$ and $\bar{p}(2)$, respectively] for a control phase of $\phi = 0$ is plotted for increasing delay time τ and normalized to the probabilities of the case without feedback:

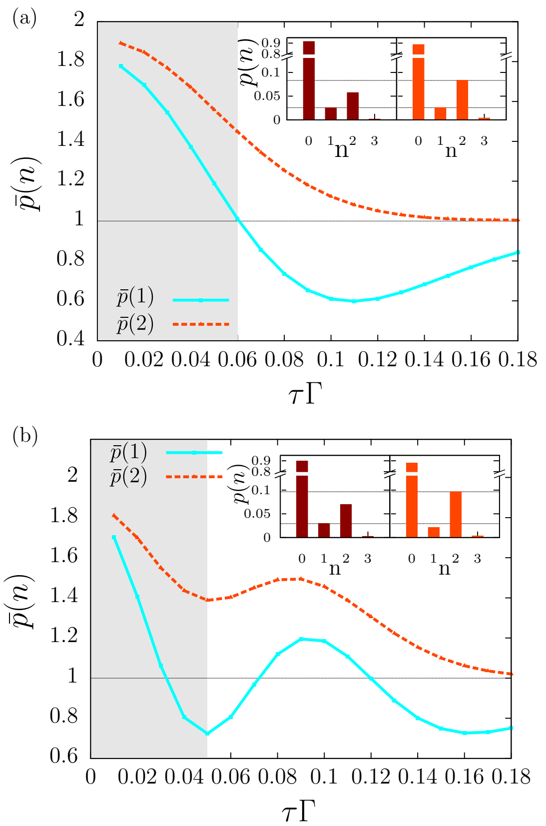

FIG. 3. Normalized probabilities $\bar{p}(n)$ [$\bar{p}(n)=1$ is the no-feedback case] for destructive feedback vs delay time τ for $A=2\pi$ and $\nu=\frac{1}{10\Gamma}\frac{1}{\sqrt{2\ln(2)}}$ (a). Two-photon emission $\bar{p}(2)\geqslant 1$ is enhanced with feedback. Inset: $p(n)$ for no feedback (red, left) and with time-delay $\tau\Gamma=0.06$ (orange, right). $p(2)$ is increased by approximately 50%. For $A=4\pi$ (b), the delay τ gives more access to control the photon statistics, due to the additional Rabi oscillation.

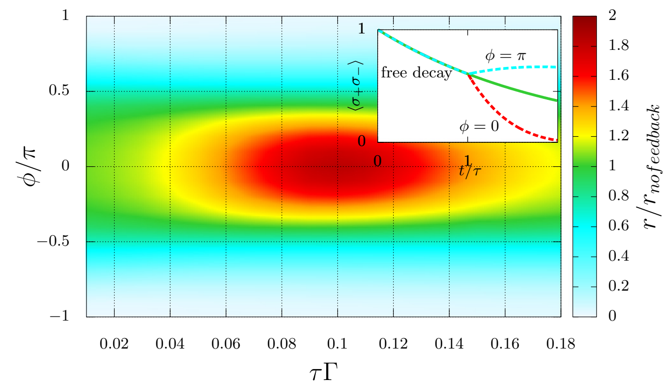

FIG. 4. Feedback-phase dependency of the normalized ratio $r=p(2)/p(1)$ at $A=2\pi$. $r/r_{\text{nofeedback}}=1$ indicates the case without feedback (green/gray). $p(1)$ dominates for $\phi=\pi$ (cyan/light gray) and $p(2)$ for $\phi=0$ (red/dark gray). Inset: Sketch for the TLS decay, for no feedback (green, solid line), for constructive feedback (cyan, dotted line), and for destructive feedback (red, dashed line).

$\bar{p}(n)=p(n)|_{\text{feedback}}/p(n)|_{\text{no feedback}}$. Therefore, a value of $\bar{p}(n)=1$ refers to the case in which feedback does not change the photon probability $p(n)$. Remarkably, one and two-photon events depend differently on the mirror distance. This allows one to enhance two-photon events without changing the probability of one-photon events (cf. Fig. 3 at $\tau\Gamma=0.06$). This observation motivates our claim that quantum Pyragas control gives access to manipulate individual photon probabilities $p(n)$, as $p(3)$ is also not changed within numerical accuracy.

To clarify this finding, we plot the photon-probability distribution for this case [cf. Fig. 3(a), inset], without feedback [Fig. 3(a), inset, left] and with feedback [Fig. 3(a), inset, right] . Clearly, we address the two-photon probability without changing the one-photon probability. This is qualitatively not expected in typical coherent quantum control setups and not within reach of Markovian quantum control, where a Lindblad dissipator governs the dynamics. Beyond this remarkable qualitative result, quantitatively the photon probabilities for two-photon events are enhanced by 50%. A further possibility for a higher degree of control over the photon statistics is to increase the amplitude of the driving laser to a pulse area of $A=4\pi$, which we show in Fig. 3(b). In general, the total photon output is increased for both cases, with feedback [Fig. 3(b), inset, left] and without feedback [Fig. 3(b), inset, right]. As only the amplitude increases, the TLS undergoes an additional Rabi oscillation on the same time scale. Thus, the same time-delay allows for more control, e.g., at $\tau\Gamma=0.05$ we increase $p(2)$ by approximately 40% and simultaneously decrease $p(1)$ by approximately 30%. Altogether, this demonstrates that a single TLS can be used to efficiently generate a two-photon state with a high degree of control [56,57]. Furthermore, it shows that non-Markovian quantum Pyragas control expands the possibilities to shape, tailor, and manipulate individual photon probabilities. A decisive difference between classical and quantum Pyragas control is the phase ϕ [cf. Eq. (2)]. In principle, the feedback phase $\phi=\omega_0\tau$ effectively triggers the spontaneous emission after delay τ and enhances or suppresses individual emission events.

If the delay is in the order of the pulse width ν, the phase is a control parameter and different results are achieved by tuning it. In Fig. 4, we discuss the impact of the phase ϕ by plotting the normalized ratio $r=p(2)/p(1)$ for different delay times τ and phases ϕ. If $r/r_{\text{nofeedback}}=1$ (Fig. 4, green/gray), the case without feedback is reproduced. We observe that two-photon emission is dominant for $\phi\in[-\pi/2,\pi/2]$, which is the destructive case where spontaneous emission is increased (see inset Fig. 4, red, dashed). The influence of this phase is most easily seen in the case of spontaneous emission without a driving field. The analytical solution from $[\tau,2\tau]$ reads

$$\langle\sigma_+\sigma_-(t)\rangle = e^{-2\Gamma t}+e^{-\Gamma(2t-\tau)}(\Gamma t-\Gamma\tau)[2\cos(\omega_0\tau) + (\Gamma t-\Gamma\tau)e^{\Gamma\tau}]. \quad (23)$$

For short delays and $\Gamma t\ll 1$, the phase has a strong impact (cf. inset Fig. 4). For $\phi\in[\pi/2,3\pi/2]$ the feedback is constructive, resulting in a suppression of spontaneous emission (cyan, dotted line). For the driven case, we note that then $p(2)$ is suppressed and $p(1)$ dominates. The phase ϕ represents fast oscillations and is more sensitive to the distance in comparison to τ. For a typical quantum dot with a band gap of 1 eV, destructive interference is robust for $\Delta L\approx 0.3\ \mu$m. For an exemplary superconducting circuit of

$\omega_0/2\pi = 6$ GHz [58], two-photon enhancement is robust for $\Delta L \approx 1.3$ cm. Instead of changing the distance, we propose also to change the TLS transition frequency to tune in and out of destructive interference as it is accessible in, e.g., superconducting circuits [58,59].

V. CONCLUSION

Our findings demonstrate the wide range of Pyragas control deep into the quantum regime where quantum interference between the photon-field and the two-level system results in a higher probability of two-photon emission compared to the case without feedback while at the same time the one-photon probability is not changed. By using time delay τ, which is tunable by the feedback geometry, as an additional control parameter, we propose a controllable setup for manipulating and tailoring parts of the photon statistics which opens up new possibilities for quantum-optical spectroscopy [60]. For short delay times, single- and two-photon emissions increase simultaneously due to a globally, on-the-fly increased decay rate. For a delay in the order of the pulse width, single- and two-photon emissions respond differently to the feedback control. This allows us to achieve a two-photon enhancement of up to 50%. Higher-pulse areas give more access to feedback control, resulting in a more efficient and pure two-photon source.

ACKNOWLEDGMENTS

We thank Florian Katsch for helpful discussions. The authors gratefully acknowledge the support of the Deutsche Forschungsgemeinschaft (DFG) through Project B1 of the SFB 910 and of the School of Nanophotonics (SFB 787).

L.D. and N.L.N. are contributed equally to this work.

[1] J. Bechhoefer, Rev. Mod. Phys. **77**, 783 (2005).
[2] E. Schöll and H. G. Schuster, *Handbook of Chaos Control* (Wiley & Sons, New York, 2008).
[3] A. Isidori, *Nonlinear Control Systems* (Springer-Verlag, Berlin, 2013).
[4] S. Boccaletti, C. Grebogi, Y.-C. Lai, H. Mancini, and D. Maza, Phys. Rep. **329**, 103 (2000).
[5] H. K. Khalil, *Nonlinear Control* (Pearson, New York, 2015).
[6] E. Schöll, S. H. Klapp, and P. Hövel, *Control of Self-Organizing Nonlinear Systems* (Springer, New York, 2016).
[7] K. Pyragas, Phys. Lett. A **170**, 421 (1992).
[8] S. Bielawski, D. Derozier, and P. Glorieux, Phys. Rev. E **49**, R971(R) (1994).
[9] S. Schikora, P. Hövel, H.-J. Wünsche, E. Schöll, and F. Henneberger, Phys. Rev. Lett. **97**, 213902 (2006).
[10] B. Fiedler, S. Yanchuk, V. Flunkert, P. Hövel, H.-J. Wünsche, and E. Schöll, Phys. Rev. E **77**, 066207 (2008).
[11] S. Schikora, H.-J. Wünsche, and F. Henneberger, Phys. Rev. E **83**, 026203 (2011).
[12] T. Erneux and P. Glorieux, *Laser Dynamics* (Cambridge University, Cambridge, England, 2010).
[13] N. Oliver, T. Jüngling, and I. Fischer, Phys. Rev. Lett. **114**, 123902 (2015).
[14] D. J. Gauthier, D. W. Sukow, H. M. Concannon, and J. E. S. Socolar, Phys. Rev. E **50**, 2343 (1994).
[15] J. Unkelbach, A. Amann, W. Just, and E. Schöll, Phys. Rev. E **68**, 026204 (2003).
[16] F. Schneider, R. Blittersdorf, A. Förster, T. Hauck, D. Lebender, and J. Müller, J. Phys. Chem. **97**, 12244 (1993).
[17] D. Biswas, T. Banerjee, and J. Kurths, Phys. Rev. E **94**, 042226 (2016).
[18] T. Banerjee and D. Biswas, *Time-Delayed Chaotic Dynamical Systems: From Theory to Electronic Experiment* (Springer, New York, 2017).
[19] T. Fukuyama, H. Shirahama, and Y. Kawai, Phys. Plasmas **9**, 4525 (2002).
[20] E. Gravier, X. Caron, G. Bonhomme, T. Pierre, and J. Briancon, Eur. Phys. J. D **8**, 451 (2000).
[21] C. Gardiner and P. Zoller, *Quantum Noise* (Springer-Verlag, Berlin, 2004).
[22] C. P. Koch, J. Phys.: Condens. Matter **28**, 213001 (2016).
[23] C. Sayrin, I. Dotsenko, X. Zhou, B. Peaudecerf, T. Rybarczyk, S. Gleyzes, P. Rouchon, M. Mirrahimi, H. Amini, M. Brune *et al.*, Nature (London) **477**, 73 (2011).
[24] P. Campagne-Ibarcq, E. Flurin, N. Roch, D. Darson, P. Morfin, M. Mirrahimi, M. H. Devoret, F. Mallet, and B. Huard, Phys. Rev. X **3**, 021008 (2013).
[25] H. Wiseman and G. Milburn, *Quantum Measurement and Control* (Cambridge University, Cambridge, England, 2006).
[26] J. Zhang, Y.-x. Liu, R.-B. Wu, K. Jacobs, and F. Nori, Phys. Rep. **679**, 1 (2017).
[27] A. Carmele, J. Kabuss, F. Schulze, S. Reitzenstein, and A. Knorr, Phys. Rev. Lett. **110**, 013601 (2013).
[28] A. L. Grimsmo, Phys. Rev. Lett. **115**, 060402 (2015).
[29] H. Pichler and P. Zoller, Phys. Rev. Lett. **116**, 093601 (2016).
[30] J. Kabuss, F. Katsch, A. Knorr, and A. Carmele, J. Opt. Soc. Am. B **33**, C10 (2016).
[31] Z. Wang and A. H. Safavi-Naeini, Nat. Commun. **8**, 15886 (2017).
[32] N. L. Naumann, S. M. Hein, A. Knorr, and J. Kabuss, Phys. Rev. A **90**, 043835 (2014).
[33] M. Rossi, N. Kralj, S. Zippilli, R. Natali, A. Borrielli, G. Pandraud, E. Serra, G. Di Giuseppe, and D. Vitali, Phys. Rev. Lett. **119**, 123603 (2017).
[34] S. M. Hein, F. Schulze, A. Carmele, and A. Knorr, Phys. Rev. A **91**, 052321 (2015).
[35] J. Gough, Phys. Rev. E **90**, 062109 (2014).
[36] R. Cook, D. Schuster, A. Cleland, and K. Jacobs, Phys. Rev. A **98**, 013801 (2018).
[37] S. M. Hein, F. Schulze, A. Carmele, and A. Knorr, Phys. Rev. Lett. **113**, 027401 (2014).
[38] Y. Lu, N. L. Naumann, J. Cerrillo, Q. Zhao, A. Knorr, and A. Carmele, Phys. Rev. A **95**, 063840 (2017).
[39] M. Kraft, S. M. Hein, J. Lehnert, E. Schöll, S. Hughes, and A. Knorr, Phys. Rev. A **94**, 023806 (2016).
[40] N. Német and S. Parkins, Phys. Rev. A **94**, 023809 (2016).
[41] J. Lindkvist and G. Johansson, New J. Phys. **16**, 055018 (2014).

[42] K. A. Fischer, L. Hanschke, J. Wierzbowski, T. Simmet, C. Dory, J. J. Finley, J. Vuckovic, and K. Muller, Nat. Phys. **13**, 649 (2017).
[43] K. A. Fischer, L. Hanschke, J. J. Finley, K. Müller, and J. Vučković, Quantum Sci. Technol. **3**, 014006 (2018).
[44] R. Lang and K. Kobayashi, IEEE J. Quantum Electron. **16**, 347 (1980).
[45] P. Bushev, D. Rotter, A. Wilson, F. Dubin, C. Becher, J. Eschner, R. Blatt, V. Steixner, P. Rabl, and P. Zoller, Phys. Rev. Lett. **96**, 043003 (2006).
[46] F. Albert, C. Hopfmann, S. Reitzenstein, C. Schneider, S. Höfling, L. Worschech, M. Kamp, W. Kinzel, A. Forchel, and Ido Kanter, Nat. Commun. **2**, 366 (2011).
[47] C. Schön, E. Solano, F. Verstraete, J. I. Cirac, and M. M. Wolf, Phys. Rev. Lett. **95**, 110503 (2005).
[48] M. T. Manzoni, D. E. Chang, and J. S. Douglas, Nat. Commun. **8**, 1743 (2017).
[49] A. Strathearn, P. Kirton, D. Kilda, J. Keeling, and B. W. Lovett, Nat. Commun. **9**, 3322 (2018).
[50] S. Hughes, Phys. Rev. Lett. **98**, 083603 (2007).
[51] Y.-L. L. Fang and H. U. Baranger, Phys. Rev. A **91**, 053845 (2015).
[52] N. Trautmann and G. Alber, Phys. Rev. A **93**, 053807 (2016).
[53] F. M. Faulstich, M. Kraft, and A. Carmele, J. Mod. Opt. **65**, 1323 (2018).
[54] A. Thoma, P. Schnauber, M. Gschrey, M. Seifried, J. Wolters, J.-H. Schulze, A. Strittmatter, S. Rodt, A. Carmele, A. Knorr *et al.*, Phys. Rev. Lett. **116**, 033601 (2016).
[55] U. Schollwöck, Ann. Phys. **326**, 96 (2011).
[56] P. R. Sharapova, K. H. Luo, H. Herrmann, M. Reichelt, C. Silberhorn, and T. Meier, Phys. Rev. A **96**, 043857 (2017).
[57] A. Gonzalez-Tudela, F. P. Laussy, C. Tejedor, M. J. Hartmann, and E. Del Valle, New J. Phys. **15**, 033036 (2013).
[58] A. Wallraff, D. I. Schuster, A. Blais, L. Frunzio, R.-S. Huang, J. Majer, S. Kumar, S. M. Girvin, and R. J. Schoelkopf, Nature (London) **431**, 162 (2004).
[59] M. H. Devoret and R. J. Schoelkopf, Science **339**, 1169 (2013).
[60] M. Kira, S. Koch, R. Smith, A. Hunter, and S. Cundiff, Nat. Phys. **7**, 799 (2011).